28 GHz Millimeter-Wave Channel Models in Urban Microcell Environment Using Three-Dimensional Ray Tracing

Jae-Hyun Lee, *Student Member, IEEE*, Jeong-Sik Choi, Jung-Yong Lee, *Student Member, IEEE*, and Seong-Cheol Kim, *Senior Member, IEEE*

***Abstract*—The millimeter-wave (mmWave) band has attracted great attention as promising spectrum for the next-generation cellular systems. However, mmWave communication systems have encountered several challenges because of different electromagnetic characteristics compared with existing spectrum below-6 GHz systems. In order to evaluate the technical feasibility of mmWave provision, 28 GHz mmWave band channel models were presented by developing an efficient three-dimensional (3-D) ray-tracing simulation. The accuracy of 3-D ray-tracing simulation was verified by comparing its results with actual measurements. The path loss (PL) agreed well in both line-of-sight (LOS) and non-line-of-sight (NLOS) regions, whereas the shadowing factor exhibited differences in the NLOS regions. The contributions of this work include confirmation of the applicability of single- and dual-slope LOS and NLOS PL models with different threshold distances for NLOS regions with low root-mean-square errors.**

***Index Terms*—28 GHz, fifth generation (5G), millimeter-wave (mmWave) communication, mmWave propagation, ray tracing.**

I. Introduction

UTILIZATION of a millimeter-wave (mmWave) frequency band is considered to be one of the most promising technologies to support the soaring demand for mobile data traffic [1]. Among the potential mmWave bands, the 28 GHz band is considered to be practical for use in the fifth-generation (5G) cellular systems [2]. However, some doubts still remain about the feasibility of the mmWave cellular system because there are considerable differences in the propagation characteristics between mmWave and the ultrahigh frequency band (300 MHz to 3 GHz). For instance, the free-space path loss (FSPL) is much higher for mmWave transmission, which severely reduces cell coverage. The mmWave band is also regarded as vulnerable to shadowing effects, resulting in worse channel quality and more outages for non-line-of-sight (NLOS) regions [3].

To ensure the success of such systems, a precise study of the radio propagation channel should be performed before cell deployment. One way to evaluate the channel characteristics is to measure the channel impulse responses at various receiver (Rx) locations. However, the ability to obtain the channel impulse responses in outdoor environments is limited because field measurements are both site-specific and time-consuming.

Ray-tracing simulations, on the other hand, are widely adopted to estimate indoor and outdoor radio channels, alleviating the burden of extensive field measurement campaigns [4], [5]. In this study, a new ray-tracing simulation tool based on the vertical-plane-launch (VPL) method was developed to study the mmWave communication channel in an urban microcell environment [6]. Our simulator is designed to calculate vertical and horizontal diffraction, which are important when simulating outdoor wireless channels, and the simulation accuracy was verified with the comparison between simulated and measured data of the high-rise urban microcell environment of Daejeon, South Korea.

II. Simulation Model

A. Wave Propagation Models Using VPL Method

The VPL method is a three-dimensional (3-D) ray-tracing method and was initially proposed in 1998 by Liang and Bertoni to simulate the 3-D radio propagation channel in efficient way [6]. Our ray-tracing simulator efficiently finds meaningful paths by dividing the simulation space into vertical and horizontal planes, while established simulators emit rays in all azimuth and elevation angles, resulting in exponential growth in computation time. First, rays are launched in the horizontal direction, which is the same as existing 2-D pincushion method, as shown in Fig. 1. These rays represent the vertical planes that contain all of the elevation angles at which rays are launched from the source point. When the vertical plane hits the wall, it is divided into two planes—one that passes or diffracts over the building wall and another that is reflected in the direction of specular reflection.

After considering the propagation of the vertical planes in the horizontal domain, the path between a transmitter (Tx) and an Rx is calculated in the vertical domain in deterministic way. The

Manuscript received November 5, 2017; revised December 18, 2017; accepted January 11, 2018. Date of publication January 15, 2018; date of current version March 1, 2018. This work was supported by the National Research Foundation of Korea funded by the Korea government (MSIP) under Grant NRF-2015R1A2A2A03008195. *(Corresponding author: Seong-Cheol Kim.)*

J.-H. Lee, J.-Y. Lee, and S.-C. Kim are with the Department of Electrical and Computer Engineering and the Institute of New Media and Communications, Seoul National University, Seoul 151–744, South Korea (e-mail: sacrifice57@maxwell.snu.ac.kr; fire3420@maxwell.snu.ac.kr; sckim@maxwell.snu.ac.kr).

J.-S. Choi is with the Intel Labs, Intel Corp., Santa Clara, CA 95054 USA (e-mail: jeongsik.choi@intel.com).

Digital Object Identifier 10.1109/LAWP.2018.2793872

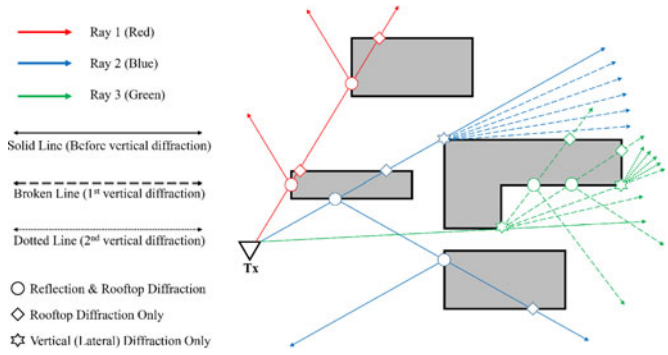

Fig. 1. Rays generated in the horizontal plane using the VPL method.

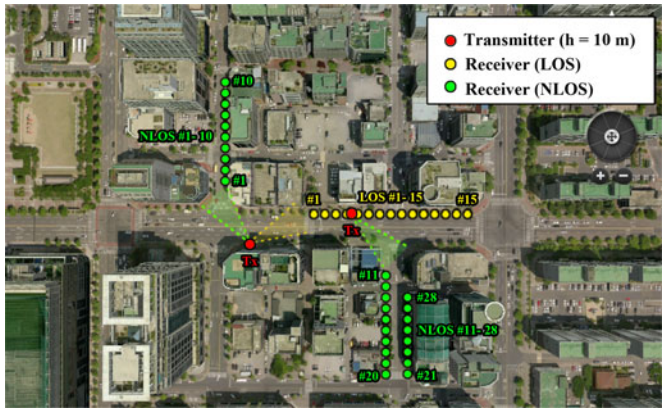

Fig. 2. Measurement points and Tx points in Daejeon. The yellow and green circles indicate the LOS and NLOS Rx points, respectively [7].

rays are considered to reach Rx when they cross the Rx capture circle within the vertical wedge. Using the vertical wedge concept, the regions that cannot be reached from the horizontal rays are readily excluded, so the VPL method can reduce computation time by calculating only valid paths. When a ray reaches Rx, the unfolded paths and all of the reflection and diffraction coefficients are calculated and recorded.

B. 3-D Building Models

To simulate the mmWave channel in the same area, we obtained geographic information system (GIS) data in the ESRI shapefile format from the Spatial Information Industry Promotion Institute, an organization affiliated with the Ministry of Land, Infrastructure and Transport, South Korea. The ESRI shapefile format is a geospatial vector data format widely used for GIS and industrial software. The building data encompasses various 3-D information such as the coordinates of complex polygonal structures and the multiple heights of buildings based on absolute elevation. However, the shapefile does not contain small obstructions such as trees, cars, and lamp posts. Detailed GIS data, such as exact coordinates, absolute altitudes, and numbers of building stories in urban areas, were obtained by parsing the shapefile.

C. Point-Wise Comparison With Measurements

To verify the performance of the ray-tracing simulator, the simulation results were initially compared with actual mmWave channel measurements. Park *et al.* [7] reported 28 GHz mmWave channel measurements obtained using the ETRI mmWave band channel sounding system. In the measurements, 30° half-power-beamwidth (HPBW) horn antennas were used for Tx, and both 10° HPBW horn antennas and omnidirectional antennas were used for Rx. The omnidirectional antennas were used to obtain path losses (PLs) in a nearby area. The measured data with directional antennas were obtained by rotating the orientation of antennas and synthesized to obtain omnidirectional PL characteristics.

The measurement site was a typical urban microcell environment composed of 7–11 story buildings (20–35 m high) with 24–35 m wide streets between buildings, as explained in [7]. The relative permittivity of building materials in ray tracing was assumed to be 6, which provides the best results for the NLOS regions [8]. Two Tx and 28 Rx locations the same as

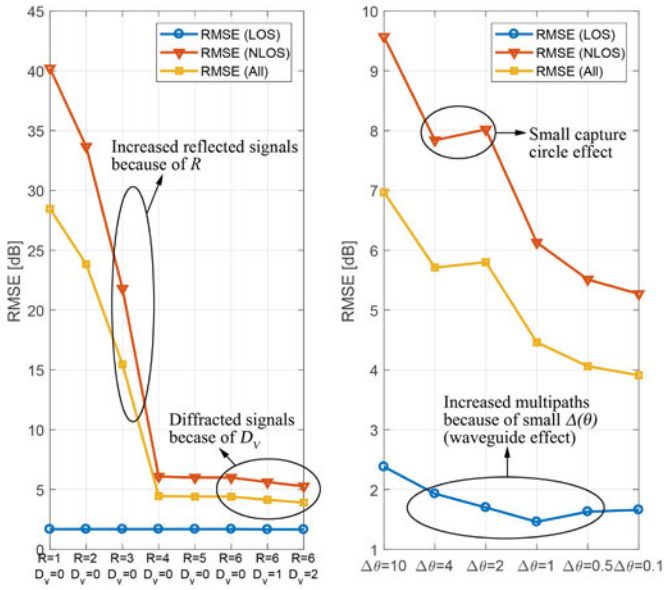

Fig. 3. RMSE results for various R, D_V , and $\Delta\theta$.

measurement locations were selected to compare measured and simulated data to find valid parameters for the ray-tracing simulation, as shown in Fig. 2. In particular, the maximum number of reflections (R), the vertical diffractions (D_V), and the beam spacing ($\Delta\theta$) have been studied through repeated comparisons, whereas these tradeoffs have not been studied extensively in previous studies on mmWave ray tracing.

Fig. 3 represents the root-mean-square error (RMSE) values of the simulation results based on the measured data for overall line-of-sight (LOS) and NLOS positions in Fig. 2. RMSE is the standard deviation of the differences in dB between measured PLs and predicted ones that are the complex sum of the received rays within 30 dB from the strongest ray path. As shown in Fig. 3, the simulation results were the closest to the measured results, when R and D_V are 6 and 2, respectively. As R increased, the number of reflected multipaths reaching the Rx position increased, so the magnitude of the PL gradually decreased. In addition, Fig. 3 also showed that RMSE of NLOS regions employing the vertical ($D_V = 1$ or 2) and horizontal diffractions is smaller than RMSE considering only the

TABLE I
HIGH-RISE URBAN ENVIRONMENT SIMULATION PARAMETERS

Simulation region	Downtown Daejeon, South Korea
Simulation range	800 m × 800 m
Number of buildings	413
Number of Tx points	2
Number of Rx	2532
Spacing between Rx	10 m grid
Height of Rx	1.5 m above ground
Beam spacing	0.1° in azimuth angle
Receivable power range	30 dB less than the strongest path
Max no. of reflections	6
Max no. of V-diffractions	2
Max no. of H-diffractions	4

horizontal diffraction ($D_V = 0$). Although the diffracted waves are substantially weaker than the direct or reflected waves, the vertically diffracted waves also affect the total PL because a significant number of diffracted waves occur at the edge of the buildings. Table I summarizes the simulation parameters for the 3-D ray-tracing simulation.

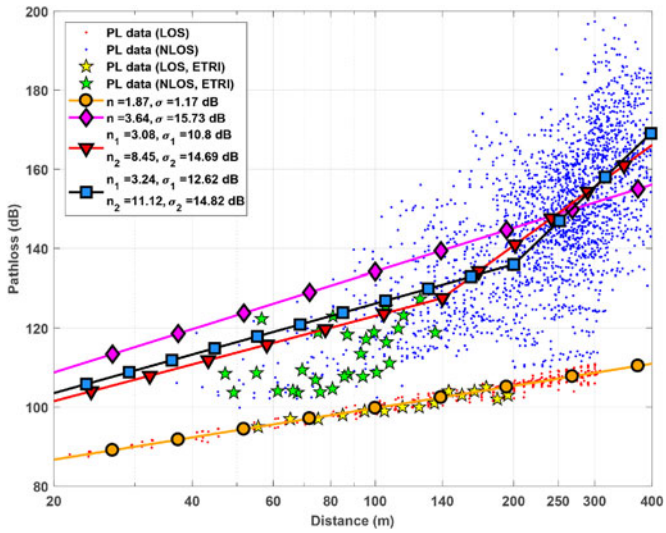

Fig. 4. LOS and NLOS PL results obtained by both measurement and simulation. The simulation covered approximately 400 m.

III. SIMULATION RESULTS

A. LOS Path Analysis

Including the measurement points, we evaluated PLs for Rx points located every 10 m along the grid lines. Among all 3600 of the Rx grid points around Tx in the center, those located inside the building were excluded; thus, 2532 street-level Rx points were simulated. For both the LOS and NLOS path analysis, the close-in free-space reference distance PL model [9] was used to compare the channel parameters and can be expressed as

$$\mathrm{PL}(f,d)[\mathrm{dB}] = \mathrm{FSPL}(f, 1\,\mathrm{m}) + 10n\log_{10}\frac{d}{1[\mathrm{m}]} + X_\sigma \quad (1)$$

where n is the path loss exponent (PLE), X_σ is a zero-mean Gaussian random variable with a standard deviation of σ in decibels, and FSPL is the free-space PL at the reference distance of 1 m, which is given by

$$\mathrm{FSPL}(f, 1\,\mathrm{m})[\mathrm{dB}] = 20\log_{10}\frac{4\pi f}{c} \quad (2)$$

where c is the speed of light.

At the LOS points, PLE was 2.1 and 1.87 for the measurements and simulation, respectively. Thus, measured PLE was higher than that of the simulation results. This finding is reasonable because the ray-tracing model incorporates multipaths with high PLs, whereas they are excluded from actual measurements because those with received power lower than the noise floor cannot be resolved. Furthermore, multipaths from sidelobe directions of the Tx horn antenna cannot reach the Rx point. However, ray-tracing includes all multipath components with powers as much as 30 dB lower than that of the strongest received signal.

From the simulated PLE results, a waveguide effect caused by the high-rise urban buildings is evident. In addition, the simulation data that are far beyond the maximum distances in [7] (180 m for LOS and 140 m for NLOS) are incorporated, including the results obtained at the actual measurement points (depicted in Fig. 4 as yellow stars). The measurement results only included the dominant LOS signals; thus, σ was 1.8 dB. Because deterministic rays were used in ray tracing and the stochastic scattering effect was not modeled, σ is only 1.17 dB, which agrees well with the measured results.

B. NLOS Path Analysis

In the NLOS regions, PLEs of 3.0 and 3.64 were obtained using the close-in PL model from the measurements and simulation, respectively. However, the single-slope PL model does not fit the results for Tx–Rx distances less than 200 m; thus, the shadowing factor soars to 15.73 dB for NLOS regions. This increase is attributable to the large quantities of Rx points extending to 400 m in both the single- and dual-slope PL models, whereas measurements were only obtained at 28 NLOS points that were locally correlated, as shown in Fig. 2. In the measurements, the Rx points were located in two adjacent areas and a directional antenna was used; therefore, the rays went through similar paths along Rx and moderate PL data were obtained.

The results indicate that the PL of an Rx point depends on the spatial environments. Even with the same Tx–Rx distance, the propagation characteristics such as the numbers of reflections and diffractions change severely depending on the location of Rx in high-rise urban microcell environment. To model the NLOS regions more accurately, dual-slope models with threshold distances d_{th} of 140–200 m were adopted in previous studies [10]. Following this method, we selected d_{th}s of 140 m (inverted red triangles) and 200 m (blue squares) for the NLOS PL model, and the results are presented in Fig. 4. It is shown that the standard deviation of dual-slope PL models is less than that of the single-slope PL model, and PLEs for distances less than 200 m become closer to the measurement results (3.08 for $d_{\mathrm{th}} = 140$ m and 3.24 for $d_{\mathrm{th}} = 200$ m). Microcells are known to have site-specific dependencies, but the dual-slope results of $d_{\mathrm{th}} = 140$ m

TABLE II
CHANNEL PARAMETERS FOR LOS AND NLOS

Models	LOS/ NLOS	d_{th} [m]	Observation range [m]	PLE (n)	σ [dB]
Measurement	LOS	–	50–180	2.1	1.8
	NLOS	–	40–140	3.0	3.8
Simulation (Single-slope)	LOS	–	50–400	1.87	1.17
	NLOS	–	20–400	3.64	15.73
Simulation (Dual-slope)	NLOS	140	20–140	3.08	10.8
			140–400	8.45	14.69
Simulation (Dual-slope)	NLOS	200	20–200	3.24	12.62
			200–400	11.12	14.82

show a better agreement than that of $d_{\mathrm{th}} = 200$ m. The results are summarized in Table II.

The σ of dual-slope models for NLOS regions within d_{th} decreased from that of single-slope model. The measurements reported lower shadowing factor, but the measurements are based on the limited data, so it is hard to represent the 28 GHz mmWave channel. On the other hand, our simulation results represent realistic PL models for 28 GHz mmWave channel in high-rise urban environment by suggesting dual-slope PL models based on the reliable 3-D ray-tracing simulation tool.

IV. CONCLUSION

This letter presented the results of 3-D ray-tracing simulations of the 28 GHz mmWave band. 3-D ray-tracing simulation requires tremendous computational overhead to account for the entire azimuth and elevation angles from Tx. Using the VPL method, a validated ray-tracing method for estimating dominant ray paths for outdoor environments, we separated the spatial domains and reduced the computational overheads without losing significant ray paths between Tx and Rx.

To verify the accuracy, the simulation results in Daejeon were compared with the measurements for the same site. Based on the comparison between the measurements and extensive simulation results, we suggested effective parametric values for the numbers of reflections and vertical and horizontal diffractions. Although the measurement result was limited, simulation results showed a good agreement with the measured data.

PLE was similar in the LOS and NLOS regions, whereas the shadowing factor in the NLOS regions exhibited a significant increase because various Rx positions within the expected radius were incorporated into our simulation to investigate the effect of multipath fading. Along with the extensive simulation results, single, and dual-slope PL models with different threshold distances were summarized to enable PL models for the 28 GHz mmWave band. The gap of the shadowing factor was attributed to the lack of measurements, which reveals the importance of ray-tracing simulations to derive realistic channel impulse responses. In addition, the observation range was increased to get more PL from the Rx point in the simulation, which was difficult for the current channel sounding systems. The data presented in this letter are expected to facilitate studies on the development of 28 GHz mmWave cellular networks in high-rise urban microcell environments.

REFERENCES

[1] T. S. Rappaport *et al.*, "Millimeter wave mobile communications for 5G cellular: It will work!" *IEEE Access*, vol. 1, pp. 335–349, 2013.
[2] M. R. Akdeniz, Y. Liu, S. Rangan, and E. Erkip, "Millimeter wave picocellular system evaluation for urban deployments," in *Proc. 2013 IEEE Globecom Workshops*, Dec. 2013, pp. 105–110.
[3] S. Rangan, T. S. Rappaport, and E. Erkip, "Millimeter-wave cellular wireless networks: Potentials and challenges," in *Proc. IEEE*, vol. 102, no. 3, pp. 366–385, Mar. 2014.
[4] J. H. Jung, J. Lee, J. H. Lee, Y. H. Kim, and S. C. Kim, "Ray-tracing-aided modeling of user-shadowing effects in indoor wireless channels," *IEEE Trans. Antennas Propag.*, vol. 62, no. 6, pp. 3412–3416, Jun. 2014.
[5] J. W. McKown and R. L. Hamilton, "Ray tracing as a design tool for radio networks," *IEEE Netw.*, vol. 5, no. 6, pp. 27–30, Nov. 1991.
[6] G. Liang and H. L. Bertoni, "A new approach to 3-D ray tracing for propagation prediction in cities," *IEEE Trans. Antennas Propag.*, vol. 46, no. 6, pp. 853–863, Jun. 1998.
[7] J. J. Park, J. Liang, J. Lee, H. K. Kwon, M. D. Kim, and B. Park, "Millimeter-wave channel model parameters for urban microcellular environment based on 28 and 38 GHz measurements," in *Proc. 2016 IEEE 27th Annu. Int. Symp. Pers., Indoor, Mobile Radio Commun.*, Sep. 2016, pp. 1–5.
[8] J. H. Lee, J. S. Choi, J. Y. Lee, and S. C. Kim, "Permittivity effect of building materials on 28 GHz mmWave channel using 3D ray tracing simulation," in *Proc. IEEE Global Commun. Conf.*, Dec. 2017, pp. 1–6.
[9] T. S. Rappaport, G. R. MacCartney, M. K. Samimi, and S. Sun, "Wideband millimeter-wave propagation measurements and channel models for future wireless communication system design," *IEEE Trans. Commun.*, vol. 63, no. 9, pp. 3029–3056, Sep. 2015.
[10] S. Hur *et al.*, "28 GHz channel modeling using 3D ray-tracing in urban environments," in *Proc. 9th Eur. Conf. Antennas Propag.*, 2015, pp. 1–5.